

# Qualifying Exam Research Report: Constraining Axion Properties Using Galaxy Cluster Spectra

Daniel Grin

## 1. Introduction

Weakly Interacting Massive Particles (WIMPs) and axions are two well motivated theoretical candidates for cold dark matter. Axions with masses in the range 3-8eV could decay to two photons, and this emission could be observed in galaxy cluster spectra. I discuss the theoretical motivation for axions and past limits on axion properties from cluster emission. I then describe my recent work, which is aimed to put constraints on axion properties using VIMOS IFU spectra of the Abell clusters 2267 and 2390. Preliminary results do not appear to improve on past constraints, though I estimate that I should do significantly better. I discuss possible reasons for this and possible directions to proceed.

## 2. Axions and the Strong CP Problem

Although the observed strong interaction obeys Charge-Parity (CP) symmetry, non-perturbative effects in QCD and weak-sector effects lead to the CP-violating term  $\frac{\theta g^2}{32\pi^2} \text{Tr}(F_{\mu\nu} \tilde{F}^{\mu\nu})$  which predicts a neutron electron dipole moment that is generically higher than experimental upper bounds (Harris et al. 1999; Baluni 1979). This Strong CP problem can be eliminated by introducing a second Higgs field, which undergoes spontaneous symmetry breaking at an energy scale  $f_{PQ}$  (Peccei and Quinn 1977). The Goldstone boson of this symmetry is called the *axion*, which interacts with fermions via  $a\bar{\Psi}\gamma_5\Psi$ . Through the triangle anomaly diagram of Fig. 1, outgoing bosons taken to be gluons, the axion interacts with gluons according to  $\mathcal{L}_{aG} = -\frac{\alpha_s}{8\pi f_{PQ}} aG\tilde{G}$ . The minimum energy configuration sets CP-violating terms equal to exactly zero. Because the axion couples to gluons and thus quarks through the strong interaction, the axion couples to the pion, and picks up an effective mass  $m_{a_{eV}} = .62 \frac{10^7 \text{ GeV}}{f_{PQ/N}}$  (Raffelt 1996). (See Fig. 2), where  $N$  is the total Peccei-Quinn charge of the leptons/quarks that couple to the axion. (Fig. 1).  $f_{PQ}$  can take on any

value high enough to set  $\theta \approx 0$  today. Taking  $10^{19} \text{ GeV} \gtrsim f_{PQ} \gtrsim 1 \text{ TeV}$  (the range between today's highest accessible energies and the Planck energy), the axion mass could theoretically lie between  $10^{-12} \text{ eV}$  and  $1 \text{ keV}$ .

## 3. Axions as Dark Matter

Axions with  $m_{a_{eV}} > 10^{-2}$  could be produced by nuclear Bremsstrahlung ( $N + \pi \rightarrow N + a$ ), come to thermal equilibrium in the early universe, and freeze out to yield an equilibrium abundance

$$\Omega_a h^2 = \frac{m_{a_{eV}}}{130} \frac{60}{g_d^*}. \quad (1)$$

After decoupling, axion temperatures and velocities fall as  $1/a$ , and their thermal velocity today would be

$$\langle v_a^2 \rangle \approx 2.7 \times 10^{-4} c \times (60/g_d^*)^{1/3} m_{a_{eV}}^{-1}, \quad (2)$$

so sufficiently massive axions will fall into cluster potentials and contribute  $\Omega_a/\Omega_m$  of the cluster mass density. Alternatively, light axions ( $m_{a_{eV}} < 10^{-2}$ ) could be produced non-thermally by non-zero  $\theta$  at early times. At the QQ phase transition, the axion field will begin to oscillate around  $\theta = 0$  and acquire a mass, yielding a cold relic density of

$$\Omega_a h^2 \approx .13 \times \Lambda_{200}^{-0.7} f(\theta_1) \theta_1^2 (m_{a_{eV}}/10^{-5})^{-1.18} \quad (3)$$

where  $\theta = \theta_1$  when axions become massive and  $\Lambda_{200}$  is the energy of the QG phase transition in units of  $200 \text{ MeV}$ . Constraints from axion cooling on stellar and red giant evolution, from the

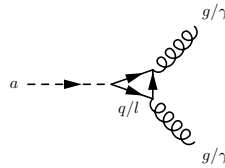


Fig. 1.— Axion coupling to gluons/photons via anomaly diagrams.

duration of neutrino bursts in supernovae, from RF cavity searches for axions, and from the requirement that have freezeout density less than the critical density, leave the axion mass windows of  $10^{-5} < m_{a_{eV}} < 10^{-3}$  and  $1 < m_{a_{eV}} < 20$ . If axions are in the upper mass range, they might be detected via line emission from galaxy clusters, while in the lower mass range, their non-thermal relic abundance would be most of the dark matter. Thus, a null result in the upper mass range is just as interesting as a detection.

#### 4. Axion Decay in Galaxy Clusters

The axion could decay to two photons either by direct coupling of standard model fermions to axions (See Fig. 1), or by a decay to pions (left half of Fig. 2), which then decay to two photons via axial vector anomalies, yielding a lifetime

$$\tau(a \rightarrow \gamma\gamma) \approx 6.8 \times 10^{24} \xi^{-2} m_{a_{eV}}^{-5} s, \quad (4)$$

where  $\xi$  parameterizes the axion-photon coupling,

$$\xi = \frac{4}{3} \left( \frac{E}{N} - 1.92 \pm .08 \right) \quad (5)$$

$N$  is defined as it is above, and  $E = 2 \sum_j X_j Q_j^2 D_j$  is a similar factor counting the number of ways the axion can directly couple to photons through quark/charged leptons,  $Q_j e$  being the electric charge of the quark/lepton and  $D_j = 1(3)$  for leptons/quarks. The stronger the coupling, the larger  $\xi$ , the higher the decay rate, and the lower the lifetime of the axion. In the DSFZ model, the standard model fermions carry PQ charge  $X_j = \mathcal{O}(1)$ . In ‘hadronic’ axion models,  $X_j = 0$  for standard model fermions, but is nonzero for exotic quarks that then couple to gluons, which couple to pions, which can then decay to photons. Thus  $\xi$  can be considerably lower in hadronic models. For  $m_{a_{eV}} > 25$ ,  $\tau < t_{Hubble}$ . If  $m_{a_{eV}} < 25$ ,

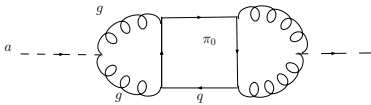


Fig. 2.— Axion mass generation via gluon coupling. The axion-gluon-gluon vertex is really an effective vertex, produced by an anomaly diagram such as in Fig. 1.

axions will have very long lifetimes, but in high density environments like clusters of galaxies, one could see line emission from axion decay. Energy/momentum conservation require each photon carry away half the axion rest-mass energy, so the wavelength of the axion line would be  $\lambda_a = 24800 \text{Å} m_{a_{eV}}^{-1}$  in the cluster restframe. For clusters with  $z_{clust} \lesssim 0.2$ , one can test for the decay of axions with  $3.3 < m_{a_{eV}} < 7.44$ , constraining  $m_{a_{eV}}^7 \xi^2$ . Because the natural linewidth  $\approx 1/\tau \approx 10^{-24} s^{-1}$  is negligible compared to the Doppler width of  $\approx 10^{19} s^{-1}$ , the spectral line will have a Gaussian profile. The measured line intensity is then given by

$$I_\lambda = \frac{6.8 \times 10^{-21} m_{a_{eV}}^7 \xi^2 \Sigma / (gcm^{-2}) e^{-\frac{(\lambda_r - \lambda_a)^2}{\lambda_a^2} \frac{c^2}{2\sigma^2}}}{\sigma_{1000} (1 + z_{cl})^4} \quad (6)$$

in units of  $\text{ergs cm}^{-2} \text{s}^{-1} \text{arcsec}^{-2} \text{Å}^{-1}$ , where  $\lambda_r$  is the cluster rest-frame wavelength being observed. Thus, one could observe the decay of thermal relic axions in the optical spectra of galaxy clusters. This idea was first implemented by Turner and collaborators (Turner 1987), using  $\mathcal{O}100$  KPNO spectra, removing sky by subtracting spectra taken at the edge of the field from spectra taken near the cluster core. No axion line was observed, and limits were put on both intracluster flux and axion coupling strength  $\xi$  by cross-correlating spectra from different clusts, identifying peaks at the requisite lag between the two cluster redshifts, and comparing their evaluated statistical significance to template spectra with axions by way of a Monte-Carlo. These limits could be improved by longer integration times, by using IFU spectroscopy to increase the coverage of a cluster, and by directly constraining  $\xi$  from the observed flux by carefully subtracting sky rather than using the more limits from cross-correlated spectra. Under the supervision of Prof. Kamionkowski, and in collaboration with A. Blain, J.P. Kneib, and G. Covone, I am using cluster spectra from the VIMOS IFU to look for axion decay emission and put better limits on the axion parameter space.

#### 5. Data

The VIMOS (VIvisible Multi-Object Spectrograph) IFU (Integral Field Unit of 1600 fibers $\times$ 4

quadrants) at VLT Melipal has been used to take spectra of Abell 2667 ( $z = .234$ ) (A2667) and Abell 2390 ( $z=0.23$ ) (Kneib et al. 2005) with 10.8 ksec exposures. I use sky-unsubtracted cubes and fit to sky, because the data pipeline estimates sky with a median at each wavelength, and thus eliminates spatially homogeneous line emission. Although the cluster mass distribution is nonuniform, this procedure would subtract out the proportion of any axion signal due to the mean cluster density, and make limits on  $\xi$  look exceedingly stringent. HST Images (F450W/5 $\times$ 2400s/F814W/4 $\times$ 1000s) of the clusters are needed to mask out parts of the IFU that fall on known cluster galaxies or background galaxies. We use images taken with HST in the filters. These images have a spatial resolution of 0".05 per pixel. Jean-Paul Kneib and collaborators have provided projected mass maps of these clusters, generated by fitting locations of giant luminous arcs and fainter multiple images in A2667/A2390 with potential parameterizations (Kneib et al. 1996). The Faber-Jackson relation and an assumed global M/L ratio were used to add the contribution of individual cluster galaxy masses. We can spatially resolve the mass distribution of the cluster, so we can weight averages over fibers to optimize regions of the IFU where an axion signal should be strongest. The advantage of looking at multiple clusters is that if a candidate line is detected, one cluster spectrum can be subtracted from the other. If a peak-trough with appropriate lag are seen, then the line may be due to axion decay in the cluster rest-frame; otherwise the line can be attributed to sky.

## 6. Data Analysis/Results

Since the VIMOS pipeline does not generate a noise estimate, I generate my own by adding Poisson counting noise to 5% of the mean flux from immediately adjacent fibers, as this is the estimated level of cross talk between adjacent IFU fibers on the VCD. Since the energy released by axion decay should come in the form of line emission, it is desirable to subtract continuum emission from the observed spectra. This is done by stepping  $\Delta\lambda = 3\frac{g}{c}\lambda_a(1+z_{cl})$  away from each candidate line location, linear fitting to continuum in  $2\times\Delta\lambda$ -sized windows on each side of this zone, and subtracting to obtain flux due only to line emis-

sion. I resample the spectral cube in wavelength to optimize signal to noise for a set of candidate axion line locations. The optimal bin size is estimated using a simple simulation run on the data cube, which varies the bin size around any candidate wavelength until signal to noise for a Gaussian line is maximized, and actual bins are then chosen to maximize the number of optimally sized wavelength bins that can be accommodated in the whole spectrum, which is resampled accordingly. To use all the information at my disposal, I express Eqn. 6 in terms of the projected surface density as measured from the weak lensing map and average over the optimal bin-size around the centroid wavelength to yield

$$\left\langle \frac{I_\lambda}{\rho} \right\rangle_{axion} = \frac{1.29 \times 10^{-18} m_{e\nu}^7 \xi^2}{\sigma_{1000} S^2(z_{cl})(1+z_{cl})^4}, \quad (7)$$

where  $S(z_{cl}) = \frac{1}{1+z_{cl}} \int_0^{z_{cl}} \frac{dz}{\sqrt{\Omega_m h^2 (1+z)^3 + \Omega_\Lambda}}$  is the dimensionless angular diameter distance to the cluster, which appears because of the conversion from density in the units of the lensing map to physical units, and  $\rho_i$  is the projected density determined by lensing. I seek to measure/constrain the quantity  $\left\langle \frac{I_\lambda}{\rho} \right\rangle$ , which should be independent of location if extra line emission is due to axion decay, and constrain the allowable values for the axion coupling strength parameter  $\xi$ . I model the emission as

$$I_{\lambda,i}^{mod} = \left\langle \frac{I_\lambda}{\rho} \right\rangle \rho_i + c_\lambda, \quad (8)$$

including a location independent sky-line emission component so that I can filter out that part of the signal which is correlated with the cluster mass density. Assuming Gaussian errors, minimizing the variance  $E_\lambda = \sum_i \frac{(I_{\lambda,i}^{mod} - I_{\lambda,i})^2}{2\sigma_{\lambda,i}^2}$  yields the standard best fit values for the slope  $\left\langle \frac{I_\lambda}{\rho} \right\rangle$  and the intercept  $c_\lambda$ , both of which turn out to be averages with weights  $\rho_i^2/\sigma_{\lambda,i}^2$  so that parts of the cluster that should contribute more signal are given greater weight. I have implemented the preceding steps in IDL to obtain  $\left\langle \frac{I_\lambda}{\rho} \right\rangle$  for A2667 in a series of wavelength bins. This sets an upper limit on  $\left\langle \frac{I_\lambda}{\rho} \right\rangle_{axion}$ , which is translated to a limit on  $\xi$  using Eqn. 7, as shown in Fig 3. The clusters fill the field of view in both our axion search and

that of Turner. So a simple comparison of collecting areas, integration times, and the fraction of cluster area masked either by our IFU masking or their choice of slit sizes and locations tells us that we should see about 300 times as many photons at a given wavelength, and thus our signal to noise should improve by a factor of  $\sqrt{300} \approx 17.8$ . Since  $I_\lambda \propto \xi^2$ , I should obtain  $\xi_{max}^{new} \approx \frac{\xi_{max}^{old}}{4}$ . Thus it is troubling that these results do not improve upon the past generation of cluster constraints in most mass bins. Several effects could be at play. Because no master-flat frame is available for the IFU, sky lines have been used to normalize the combined response function of the fibers and CCD. For the sky-unsubtracted cube, the VIPGI software which provides the data uses a procedure that normalizes discrete sub-patches of each IFU quadrant and this may introduce a spurious spatially dependent (and hence density dependent) component to the flux. My algorithm might trip up on this sort of artefact to yield a less stringent limit than ultimately possible. I'm currently investigating how to get a fiber by fiber flux normalized data cube. Also, I am resampling the spectra before I make any attempt to remove sky line emission. In a bin straddling a sky line, I could be artificially folding sky flux over into measured quantities. It may also be wise to mask the location of sky lines from the resampling algorithm even after fitting for sky, because sky fits will be imperfect. I am currently working to sort out these issues and to apply the same technique to A2390. Once this is done I can do a joint fit for my best fit parameters. Because the same sky line corresponds to different rest-frame wavelengths for the two clusters, I'll be able to constrain even those parts of the spectrum that fall on sky for a single cluster. Finally, I'm eager to extend this technique to higher redshift clusters, such as the lensing cluster RDCS 1252 at  $z = 1.237$ , as it will allow higher axion masses to be constrained in a similar fashion.

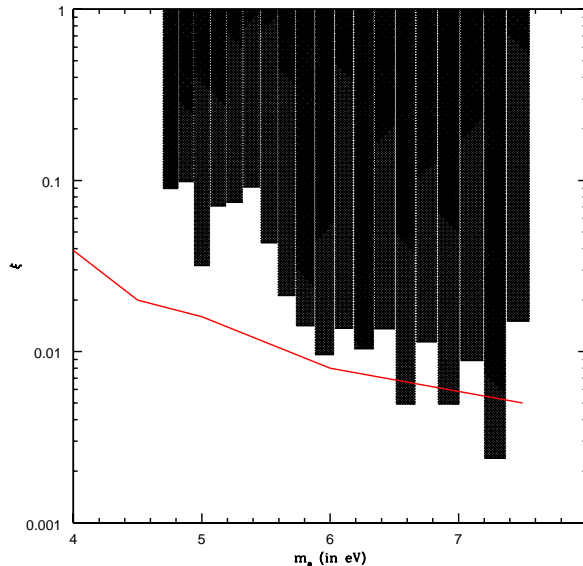


Fig 3. Excluded region from A2667 is in black. Region above red line is excluded by (Bershady 1991)

## REFERENCES

- V. Baluni, Phys. Lett. D **19**, 2227 (1979).
- Leader, E., Predazzi, E., 1996, An Introduction to Gauge Theories and Modern Particle Physics, Volume 2: CP-violation, QCD, and hard processes. Cambridge University Press, Cambridge.
- P. G. Harris *et al.*, Phys. Rev. Lett. **82**, 904 (1999).
- Peccei, R.D., Quinn, H.R, Phys. Rev. Lett. **38**, 1440 (1977). Peccei, R.D., Quinn, H.R., Phys. Rev. D **16**, 1791 (1977).
- M. A. Bershady, M. T. Ressel and M. S. Turner, Phys. Rev. Lett. **66**, 1398 (1991).
- M. S. Turner, Phys. Rev. Lett. **59**, 2489 (1987) [Erratum-*ibid.* **60**, 1101 (1988)].
- Raffelt, G.G., 1996, Stars as Laboratories for Fundamental Physics: The Astrophysics of Neutrinos, Axions, and Other Weakly Interacting Particles. The University of Chicago Press, Chicago.
- J. P. Kneib, R. S. Ellis, I. Smail, W. J. Couch and R. M. Sharples, arXiv:astro-ph/9511015.
- J. P. Kneib, G. Covone, in preparation.

---

This 2-column preprint was prepared with the AAS L<sup>A</sup>T<sub>E</sub>X macros v5.2.